Amelioration of The Dielectric Properties of Ceramic Insulators Using Nano-alumina

S. M. A. El-Gamal[1], M. A. Abd-Allah[2] ,*Eman Belal[3], T. Eliyan[2], Osama A. Desouky[4]

[1] Chemistry Department, Faculty of Science, Ain Shams, University, Cairo, Egypt
[2] Faculty of Engineering, Shoubra, Benha University, Banha, Egypt
[3] Marg Higher Institute of Engineering and Modern Technology (MIE), El Marg El Gadida, Cairo, Egypt
[4] Bilbis Higher Institute of Engineering (BHIE), Bilbis, Sharqia, Egypt
*E-mail: emanbelal2020@yahoo.com

Abstract - *Outdoor HV porcelain insulators face various environmental stresses that cause their degradation. Consequently, amelioration of their insulating properties becomes a target of recent researches to survive higher voltage levels. Investigating the impact of the addition of 0, 5, 10, and 15 wt. % nano- alumina (NA) on the dielectric and physical characteristics of porcelain materials at elevated sintering temperatures is the aim of this study. Porcelain specimens were synthesized from kaolin, feldspar, and quartz as available low-cost raw materials. The specimens were sintered at 1100, 1200, 1300, and 1400°C for 2 h. For some specimens, the microstructure and phases formed were identified using scanning electron microscopy and X-ray diffraction techniques. The changes that occur upon heating (include melting, phase transition, sublimation, and decomposition) were identified by Differential Thermogravimetric Analysis. The dielectric strength, relative permittivity, and loss tangent of different samples were measured at a large scale of frequencies. Breakdown strength values of different samples were verified by applying the Finite Element Method. The best electrical and physical properties were achieved at 1300ºC. At this temperature the porcelain sample containing 5 wt. % NA presented optimum physical characteristics as well as good insulating properties assent the feasibility of producing electro-technical porcelain.*

Keywords – Relative permittivity, DTA, XRD, porosity, Dielectric loss, FEM.

1. Introduction

Porcelain, glass, and polymeric composites are generally utilized as electrical insulators in HV power networks. Ceramic materials are usually operated in electrical systems because of their good electrical, mechanical, and thermal characteristics under unfavorable environmental effects [1-4]. Porcelain insulators are complex ceramic materials that are widely studied due to their advanced engineering applications [5-7]. The merits of porcelain materials over other ceramics support their usage for manufacturing large size HV insulators having complex configuration [8]. The good electrical, physical, and thermal properties of porcelain under severe environmental conditions reinforced their confidence performance in the power network and support their continued use over the centuries [9]. In recent decades great efforts have been done by many researchers to enhance these important properties [10-14]. For fulfilling these demands, many investigations focused on developing porcelain insulators having enhanced performance under severe environmental effects [15-17].

The electric characteristics of sintered porcelain are generally affected by the amount of the glassy phase formed from feldspar and quartz elements. These characteristics are determined by the mobility and amount of K^+ and /or Na^+ ions present in this phase. Increasing the glassy phase content facilitates the motion of ions (K^+ and Na^+) and thus increases their conductivity. Generally, it was reported that the existence of K^+ and Na^+ cations increases the permittivity of porcelain, while it is reduced when these cations are replaced by Ca^{2+}, Mg^{2+}, and Ba^{2+} cations. Mullite has a crystalline structure and has a central role in the electrical properties of ceramic insulators. Since, ceramics composed of clay matrix or the glassy phase, the mullite maintains the stress level higher than just in the composite matrix [18-21].

Nanotechnology represents an advanced option to enrich insulators' characteristics. Generally, there are few investigations related to nano-material applications in porcelain insulators compared to other ceramics, it is expected to be very promising and interesting insulators

[22-26]. The presence of impurities and pores causes deprivation of the insulating properties of porcelains, so good electrical porcelain insulators should be free from porosity and impurities [27].

The permittivity (ε') and the loss tangent (tan δ) of porcelain material depend on the characteristics and quantities of different phases [28-30]. The addition of NA to ceramic materials enhance their electrical, mechanical, and optical properties and so, enable their utilization in many modern industrial areas too. Aluminum oxide-based material has a significant advantage due to its hardness, chemical inactivity, high melting point, non-volatility, and resistance to corrosion and abrasion [31-33]. The properties of NA particles are largely affected by their diameter, morphology, and homogeneity [34].

Porcelain insulators make up a large base of commonly used insulators for both LV and HV insulation. Recently great efforts were paid to enrich the behavior of insulators utilized in different equipment of power networks. Important motivating points of this study are; the lack of researches concerned with investigating the influence of nanofillers on different characteristics of ceramic insulators used in power stations despite their wide applications as well as investigating the effect of sintering temperatures of nanocomposite ceramic insulators on their physical and electrical features to determine the optimum temperature for obtaining porcelain insulator having high insulating characters

2. Materials and Experimental Techniques

2.1. Starting Materials

Low-cost porcelain resources namely; Kaolin ($AL_2O_3.2SiO_2.2H_2O$), feldspar ($K_2O.AL_2O_3.6SiO_2$), and quartz (SiO_2) taken from different deposits in Sinai and Aswan (Egypt), were used in this investigation for the preparation of four porcelain samples.

Various porcelains powder was prepared as follows: firstly, mixing 25% feldspar + 50% kaolin and 25% quartz by weight. To ascertain the final homogeneity of the samples, the dry components are mixed with 1 liter of tap water and milled in a ball mill using five small porcelain balls for 3 hours. The resulting mixture was passed through a magnetic sieve of 200 μm to eliminate the iron content. Then it was cast into a rectangular mold then dried at 110◦ C for one day. Finally, grinding the specimens finely to pass through a sieve of 200 μm. The selected percentages of the raw materials used in this investigation were according to the results of different tests performed. Table (1) illustrates the composition of the prepared porcelain samples. The data of the physical characteristics obtained for all samples at different firing temperatures are given in Table 2.

Table 1. Composition of different porcelain samples

Raw material	Mixture (1)	Mixture (2)	Mixture (3)
Ball clay ($Al_2H_2O_{10}Si_3$)	50 %	0 %	0 %
Kaolin	0 %	50 %	50 %
Feldspar	35 %	25 %	30 %
Quartz	15 %	25 %	20 %

2.2 Molding

Porcelain, samples were molded as discs with 2 mm & 2 cm thickness and diameter: respectively. This was achieved by pressing a suitable mass of the wetted sample (∼8 g) by using a hydraulic piston under the pressure of 60 MPa. The specimens were dried overnight in an oven at 110 º C, then using a kiln muffle the samples were fired at 1100, 1200, 1300, and 1400 °C for 2 h. The previous steps were repeated to prepare porcelain nanocomposite specimens (porcelain sample admixed by 5, 10, and 15 wt. % of NA). Porcelain powder and the calculated amount of NA were mixed first manually in a mortar. Specimens notations and composition are given in Table (3). The details of sample preparation and tests performed were illustrated by a flow diagram displaying the Fig. (1).

Table 2. Physical characteristics of prepared samples

physical properties	Mixture (1)			Mixture (2)			Mixture (3)		
	900 °C	1220 °C	1335 °C	900 °C	1220 °C	1335 °C	900 °C	1220 °C	1335°C
Water Absorption (WA)%	5.41	2.90	1.82	1.7	1.04	0	7.36	2.89	2.90
Apparent porosity (AP)%	0.22	0.08	0.05	0.23	0.09	0	0.11	0.20	0.05
Bulk density (BD)	7.38	8.17	5.48	4.81	5.6	5.8	7.9	5.5	5.9

Table 3. Sample composition and their notations

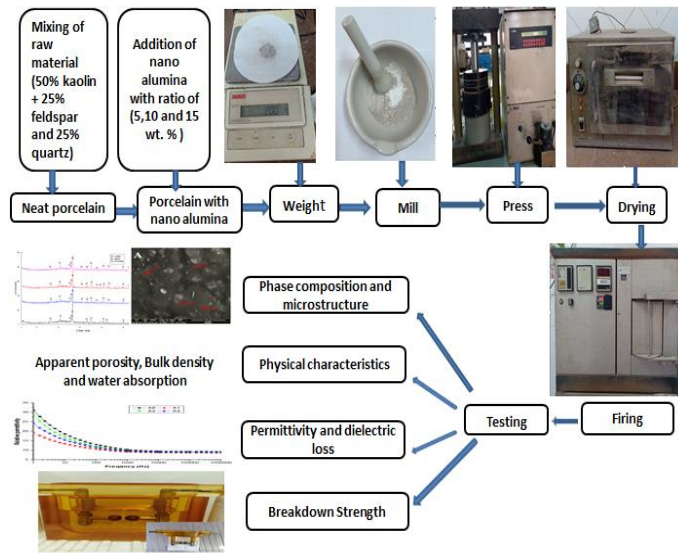| Mix	Porcelain material (Wt. %)	NA (Wt. %)
A0	100	0
A1	100	5
A2	100	10
A3	100	15

Fig. 1. The schematic diagram for samples preparation and tests performed

2.3. Characterizations

The physical characteristics of sintered porcelain and porcelain – NA composites were investigated via the determination of the apparent porosity (AB), bulk density (BD), and water absorption (WA), these parameters were determined according to Archimedes method; ASTM C20, ASTMC356-10[35, 36].

The AB, BD, and WA values were calculated according to the boiling method as follows: the sample was subjected to two-hour boiling, followed by four-hour water soaking at normal temperature, and then weighed. Then the values of WA, BD, and WA were calculated by substitution in equations (1), (2), and (3); respectively.

$$\text{Porosity=} \quad \frac{w_s - w_d}{w_s - w_{sp}} \tag{1}$$

$$\text{Bulk Density (g/ cm3)} \quad = \frac{w_d}{w_s - w_{sp}} \tag{2}$$

$$\text{Water Absorption =} \quad \frac{w_s - w_d}{w_d} \tag{3}$$

Where:

w_d = dry weight of the specimen

w_s = weight of specimen after boiling and soaking in water

w_{sp} = weight of specimen suspended in water

The dielectric properties of the sintered porcelain samples were measured using Agilent E4980A LCR device. The permittivity (ε') and the loss tangent (tan δ) of different samples were measured at a range of frequency 20 Hz to 1 MHz. The permittivity of insulating material is represented by,

$$\varepsilon_r = \varepsilon' - j\varepsilon'' \tag{4}$$

The loss tangent (tan δ) is given by,

$$\tan \delta = \frac{\varepsilon''}{\varepsilon'} \tag{5}$$

Microstructure, thermal stability and phase composition of some samples were identified using Scanning Electron Microscope (SEM), differential thermal analysis (TGA/ DTG), and X-ray diffraction analysis (XRD).

3. Results and discussion
3.1 Phase composition and microstructure
3.1.1 X-ray diffraction analysis

Different phases formed during sintering the tested samples at 1300 °C were identified using X-ray analysis technique. For blank sample (A0) the X-ray patterns obtained revealed the presence of mullite ($3AL_2O_3 . 2Sio_2$) at about ~ 2 θ =16.443 (d= 5.38674) , 2 θ =26.024 (d=3.42119) ,2 θ =26.331 (d =3.38203) , 2 θ =30.885 (d= 2.89295) , 2 θ =35.221 (d =2.54607) ,2 θ =40 .857 (2.20692) and 2 θ =50 .093 (d= 1.81953). Quartz (SiO_2) also detected by diffraction at ~ 2 θ =20.841 (d =4.25890), 2 θ =26.623 (d= 3.34558), 2 θ =39.409 (d =2.28463), 2 θ =42.479 (d= 2.12633).Fig. (2). The X-ray pattern for A1, A2 and A3 samples fired at 1300 °C for 2h displayed the same diffraction patterns as blank with the presence of the characteristic peaks of Corundum (AL_2O_3) . The XRD analysis of mixes A1-A3, displays the same diffraction patterns as blank (A0), revealing that the presence of NA did not affect the phase composition of porcelain material, Fig. (2). The XRD patterns of these mixes indicate the peaks of mullite at about 2 θ =16.535 (d=5.35689) , 2 θ =25.969 (d=3.43830) , 2 θ =26.378 (d=3.37613), 2 θ =31.015 (d=2.88105), 2 θ =33.235 (d=2.69353), 2 θ =35.272 (d=2.54251) and 2 θ =40.884 (d=2.20554). Quartz at about 2 θ =20.889(d=4.24913), 2 θ =26.665 (d=3.34034), 2 θ =50.152 (d=1.81753) and 2 θ =59.93 (1.54223). The main peaks characteristic for Corundum are detected at about 2 θ=25.677 (d=3.4660), 2 θ =37.852 (d=2.37495), 2 θ =43.451(d=2.08101), 2 θ=52.58 (d=1.73916) and 2 θ =57.51 (d=1.60124) [37-40].
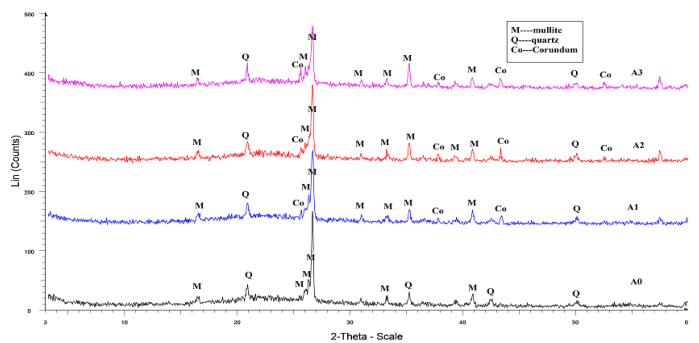

Fig.2 XRD pattern of porcelain samples sintered at 1300 °C

3.1.2 Scanning electron microscope (SEM)

The microstructure features of samples made from neat porcelain (A0) and A1 (porcelain + 5% NA) after sintering at 1200 and 1300 °C for tw0 hours were inspected by using SEM. The SEM images of specimens made from blank (A0) sintered at 1200 and 1300 °C revealed the creation of a

3

highly dense structure composed of amorphous quartz that is predicted as black and gray polyhedral grains. Besides, millet grains that dispersed in the vitreous matrix as white grains could be distinguished. The SEM pictures also confirmed the presence of some small pores along with the matrix that appears as a black region. The mean size of the identified grains is ranged between (29-87) nm and (148-186) nm, Fig. (3.a), and Fig. (3.b). The SEM images of specimens made from mix A1 after 2h sintering at 1200 and 1300°C are displayed in Fig. (3.a) and Fig. (3.b), respectively. The SEM images confirmed the attendance of the same phases and same microstructure as neat porcelain besides the appearance of white spots of corundum grains. Additionally, the SEM images revealed a highly dense matrix when compared to a blank at each firing temperatures. The dense matrix of these specimens is assigned to the presence of NA particles, referring to the nano dimensions of NA particles, it acts as a good filler, that fills the nano and micropores present along with the matrix, which causes reducing the degree of porosity of porcelain sample and this intern causes enhancing its insulating characteristics. The average size of different grains predicted was pointed along with the matrix, Fig. (4.a) and Fig. (4.b).

Fig. (3.a) SEM image of neat porcelain (A0) sintered at1200 °C

Fig. (3.b) SEM image of neat porcelain (A0) sintered at1300 °C

Fig. (4.a) SEM image of the sample (A1) sintered at1200 °C

Fig. (4.b) SEM image of the sample (A1) sintered at1300 °C

3.1.3. Differential thermogravimetric analysis (TGA/DTG)

The outcomes of the TGA/DTG analysis obtained for samples made from mixes A0-A3 treated at normal temperature are presented in Figs. (5- 8); respectively. The TGA/DTG curves of blank (A0) displayed the attendance of four endothermic peaks at a temperature of 382.5, 506.5,757, and 960 °C. The first peak located at 382.5°C is owing to the removal of the hygroscopic water. Also, the TGA/DTG curves ascertain the thermal stability of the blank sample since its melting temperature was shifted from 300 °C to higher temperature (382.5 °C), Fig. (5). The endothermic peak located at ~ 506.5°c is the major peak related to the decomposition of porcelain mineral structure (removal of combined water of porcelain mineral) and also related to the allotropic transformation of quartz. So, this endothermic process is associated with the main weight loss as an outcome of decomposition and dehydration [41, 42]. The endothermic effect located at ~757 and 960°C is related to the decomposition of any carbonates in the raw ceramic material [43]. The TGA/DTG for porcelain specimens containing 5% NA (mix A1) indicate six endothermic peaks located at a temperature of 107,223.5, 506.5,730,804, and 960 °C, Fig. (6). the first two endothermic peaks that appeared at 107 and 233.5 °C are related to the moisture loss [28]. While the main endothermic peak appeared at 506.5°c is linked to the breakdown of porcelain mineral structure and the allotropic transformation of quartz. Finally, two endothermic peaks observed at 804 and 960 °C are associated with the decomposition of any carbonates present in porcelain natural resource Fig. (6) [43]. The TGA/DTG analysis of samples prepared from porcelain material admixed with 10 and 15 NA wt.% (mixes A2, A3, respectively) presented the same thermal behavior as mix A1 (containing 5% NA) and same the endothermic peaks, Fig(7) and Fig. (8); respectively.
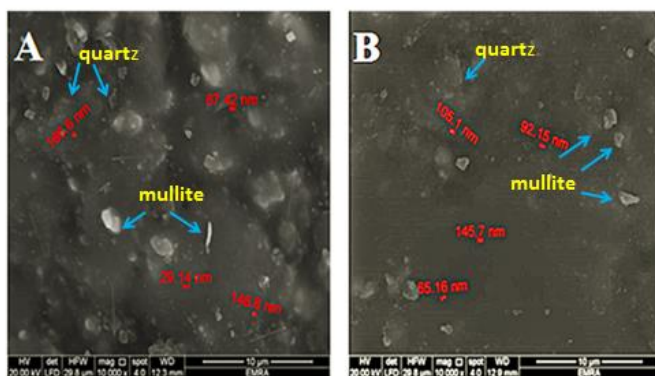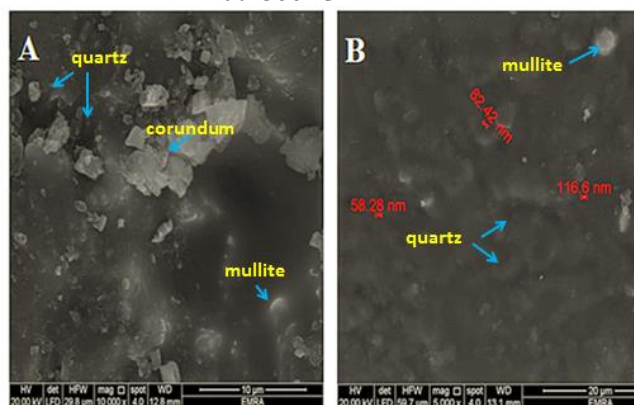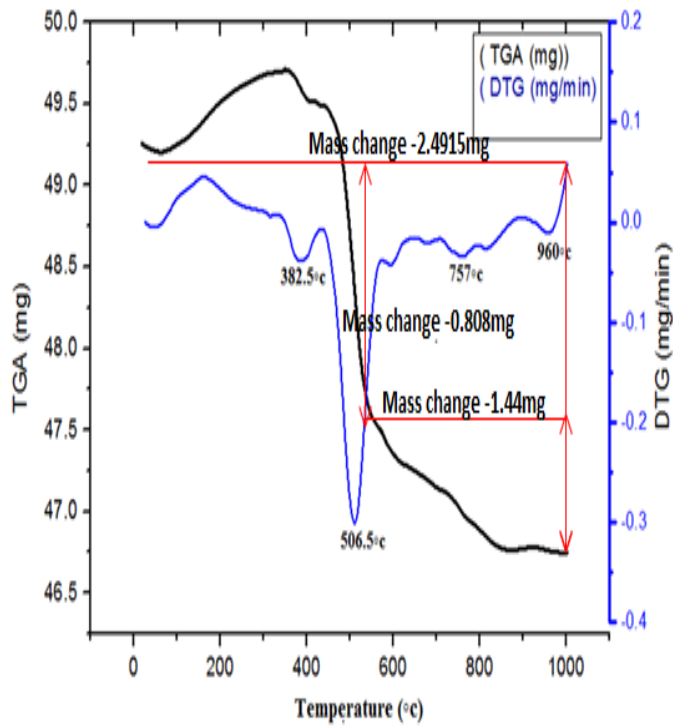
4

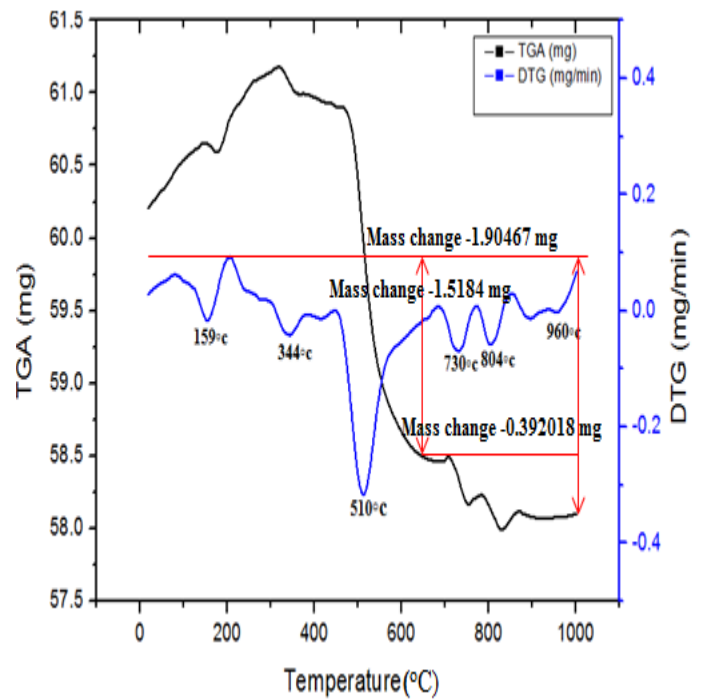**Fig.5** TGA/DTG curves of neat porcelain (mixA0)

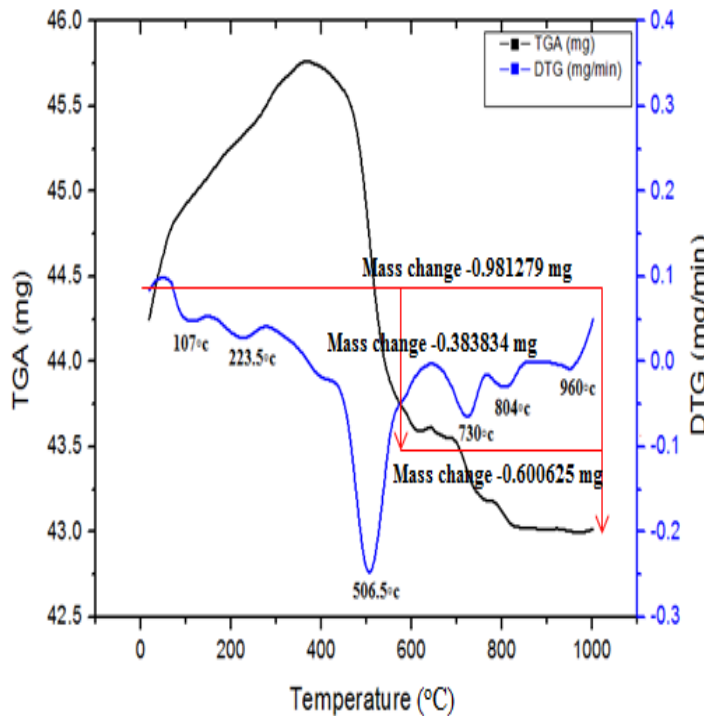**Fig.7** TGA/DTG curves of mix A2 (neat porcelain + 10%NA)

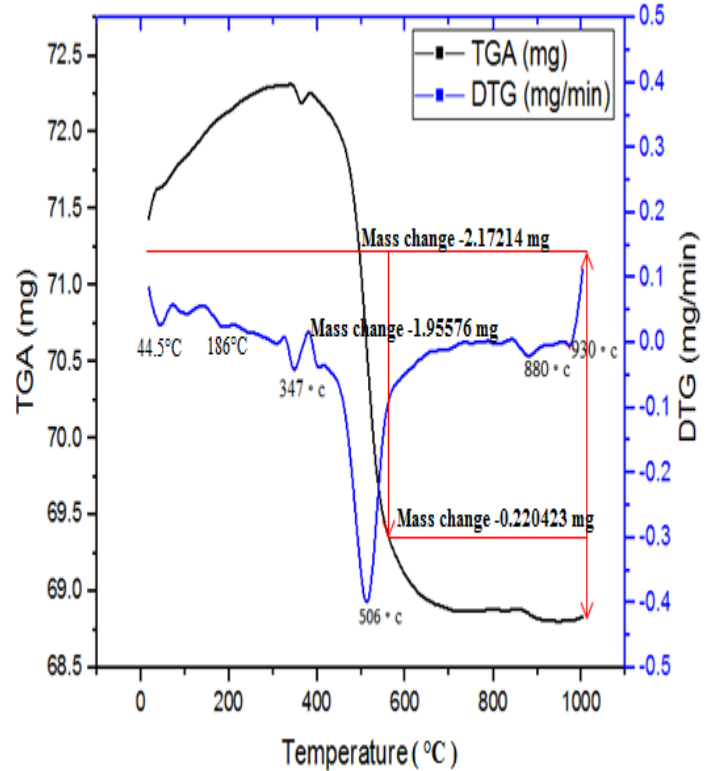**Fig.6** TGA/DTG curves of mix A1 (neat porcelain + 5%NA)

Fig.8 TGA/DTG curves of mix A3 (neat porcelain + 15%NA)

3.2 Physical characteristics

The BD, AP, and (WA) values of the tested specimens at all treated temperatures were evaluated to appraise their physical characteristics and presented in Fig. (9).

All samples showed a continuous remarkable rise in BD, a reduction in AP, and WA values with raising the firing temperature. These results imply a continuous decrease in the porosity of the sintered porcelain specimens with increasing firing temperature. Increasing the firing temperature support increase the glassy phase content in the porcelain matrix. Additionally, the BD values reflected a notable growth with increasing the NA contents (up to 15 wt. %) at all sintering temperatures. These results can be linked to the filling role of NA particles, as the outcome of the nano dimension of NA particles, NA particles can fill both the micro and nanopores appear in the porcelain matrix, which causes a notable reduction in the degree of porosity of the fired porcelain specimens and gives more compact and highly dense structure as compared to a blank (A0) [44]. Porcelain samples synthesized from Porcelain material + 5 % NA (mix A1) sintered at 1300°C display the best whole physical characteristics as related to other tested samples (BD, 3.255 g/cm3, WA, 0.218% and AP 0.099 %). These outcomes nominate this sample to be used as a perfect insulator. Since for HV insulator, WA should be minimized [45]. Similar results were stated by many researchers, Niraj Singh Mehta [46] clarifies the effect of the addition of alumina and silica on the electrical and physical features of porcelain bodies over high sintering temperatures. The results indicated that; sample having silica 10 wt.% of alumina 35 wt.% and sintered at 1350°C, shows the extreme BD of 2.55 g/cc with WA of 0.94%. In another study, porcelain samples composed of 33% Kaolin, 15% ball clay, 32% feldspar, and 20% quartz presented WA (1.55%), TP (4.64%), and BD [47]. The same results were achieved by J.E. Contreras [48] which clarifies that the addition of 1 % alumina nanoparticles to porcelain samples causes a slight rise in the BD from 2.360 to 2.382 for sintered porcelain samples. This slight increase in BD can be approved to the higher values of density of n-Al2O3 due to the very small size of nanoparticles [49].

4. Permittivity and dielectric loss

A dielectric permittivity ε_r is caused by polarization effects in the dielectric material. Except for the polarization distortion of insulating material (ionic, lattice polarization, and electronic), the direction of polarization is of great impact, as much molecular structure of insulating materials has stable dipoles. This is the major reason for the polarization losses. Also, this is accountable for the frequency dependence of ε_r and tanδ, which is important for technical applications. The electrical networks are exposed to overvoltages, which are classified into internal and external overvoltages. These overvoltages include a wide range of frequencies when resolved by Fourier analysis. So, the dielectric constant and the dielectric loss must be determined for this range which begins with the power frequency to the ultra-high frequency.
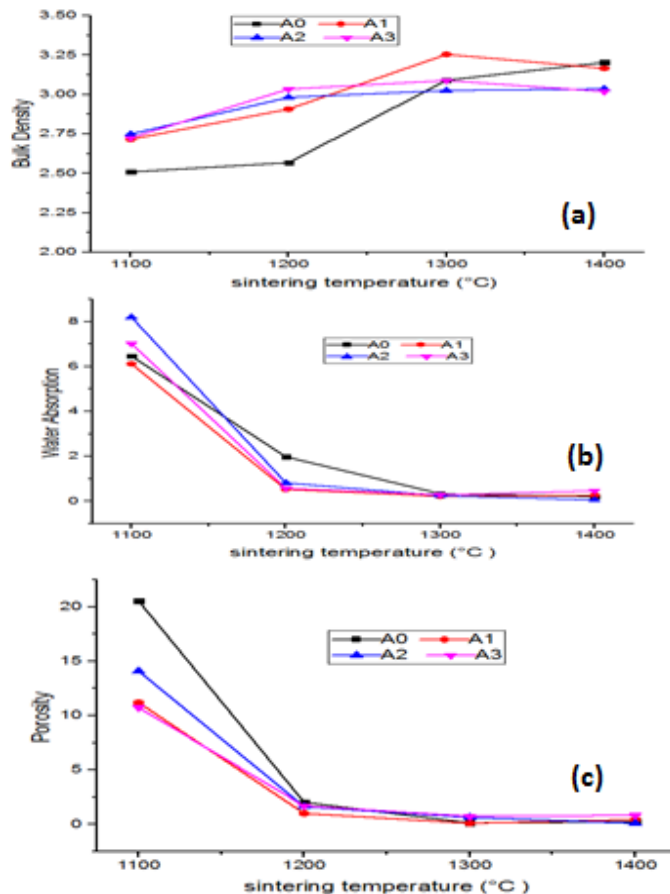

Fig.9 Physical features of different porcelain samples at various sintering temperatures:
(a)Bulk density, (b) Water absorption (c) apparent porosity

Nano-Alumina particles are added with a different concentration on the blank samples and burning at sintering temperatures ranged from 1100 ᵒC to 1300 ᵒC. For each sample, the permittivity and dielectric loss were measured. The measured values displayed that the permittivity of porcelain samples with the different addition of NA is reduced compared to the blank sample, as shown in Fig. (10.a) and Fig. (11.a). It is observed that, the permittivity for samples with 5wt. % NA at firing temperature 1200 ᵒC is 11.4, compared with neat porcelain, which is 14.3. When the samples sintered at 1300 ᵒC the relative permittivity for samples with 5wt.% nano-alumina addition reaches 7.2 compared with the blank sample, which is 9.33. The outcomes are indicated that the permittivity decreases with increasing the sintering temperature. These results can be explained as follows; as the firing temperature increased, the glassy phase content in the porcelain matrix will be increased. Additionally, the bulk density values showed a notable increase with increasing the NA contents (up to 15 wt. %) at all sintering temperatures. These results nominate

6

these porcelain - NA composites to be used as good solid insulators in power networks, since for HV insulators, water absorption of porcelain insulators, should be minimized or zero [45].

One of the basic elements responsible for the goodness of the insulating materials is the dielectric loss (Tan δ). The results clearly showed that, the porcelain sample with 5 wt. %. nano-alumina has high values at low frequencies. As the frequency increased tanδ is decreased. At power frequency (50 Hz) tan δ reaches about 0.162 while the blank has a value of 0.25 at sintering temperature 1200 °C. At 1300 °C, tan δ of the nanocomposite material decreases to about 0.0116, while the tan δ of the blank is about 0.0168, as displayed in figs. (10b, 11b).
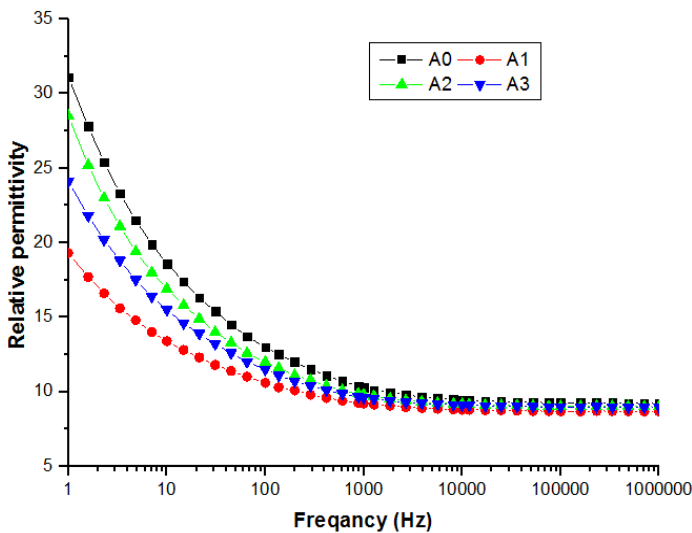

Fig. (10. a) Relative permittivity (ε_r) across frequency for porcelain insulator with nano Alumina adding at sintering temperature 1200 °C
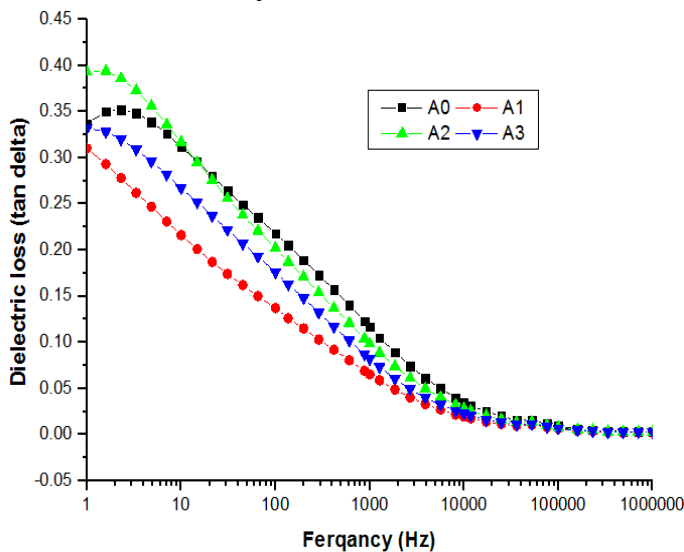

Fig. (10. b) Dielectric loss across frequency for porcelain insulator with nano Alumina adding at sintering temperature 1200°C

Fig. (11. a) Relative permittivity (ε_r) across frequency for porcelain insulator with nano Alumina adding at sintering temperature 1300 °C

Fig. (11. b) Dielectric loss across frequency for porcelain insulator with nano Alumina adding at sintering temperature 1300°C
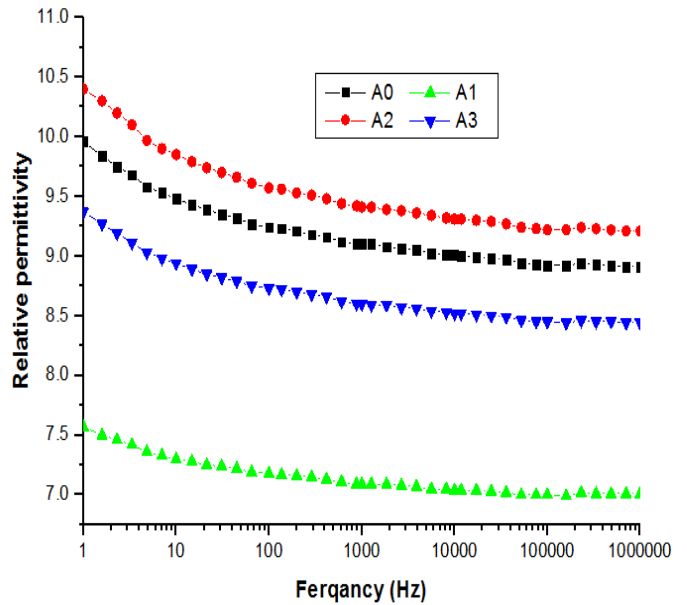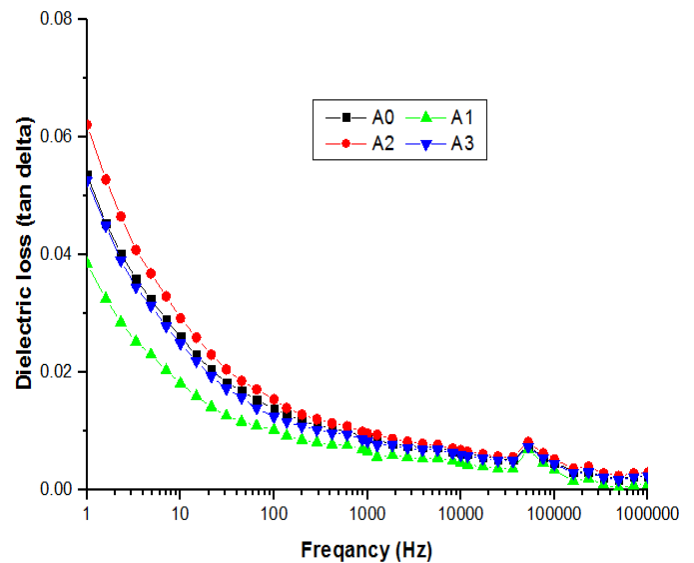
5. Breakdown Strength

Breakdown strength is a considerably important property for insulating systems whereas the dimension of the insulating system depends on electric field values. The breakdown test is conducted with an AC voltage, which should be increased smoothly from zero to the breakdown value. The average value of the breakdown voltage is determined from 5 trials. The breakdown strength can be evaluated from the breakdown voltage and the smallest electrode spacing. The AC breakdown voltages (AC-BDV) of the different samples were measured using an electrode

7

arrangement of sphere-to-sphere test cells agreeing to ASTM (D149-09) standard.

The porcelain with different adding of nano-alumina filler was tested and their AC-BDV was determined and related with the blank sample, all sintered at 1200 ℃ and 1300 ℃. The average value of the AC-BDV of the blank sample sintered at 1200 ℃ was 21.87 kV. It is noticed that the AC-BDV was raised with the addition of nano-alumina. The samples of porcelain with 5% nano alumina addition achieved the peak value of average AC-BDV (27.5 kV). With additions of 10%, 15% nano Alumina, a significant decrement in AC-breakdown voltage was observed, as displayed in Fig. (12). Fig. (13.a) and Fig. (13.b) show the potential and electric field distributions in and around the sample of porcelain with 5wt% nano Alumina (A1), which have the maximum simulated and measured AC-BDS. These results agree with other results reported by other researchers. J.E. Contreras presented a study of the impact of alumina nanoparticles on the insulator capacity of the siliceous porcelain. It is noticed that nano-alumina enhanced the dielectric strength of the electric porcelain. As by addition of α-Al2O3 nanoparticles by a ratio of (1wt. %) breakdown voltage increases by 27.7% [48]. Nano alumina addition has an actual task in the dielectric features of pure porcelain as dielectric strength increased and dielectric constant decreases. When increased the percentage of nano alumina adding, the dielectric constant decrease this may be owing to of increased mullite phase and decrease of quartz that mean decrease in the glass phase where quartz and glass are insulators at area temperature by themselves but mullite may be a more conducting phase because mullite contains O2 in structure [50].
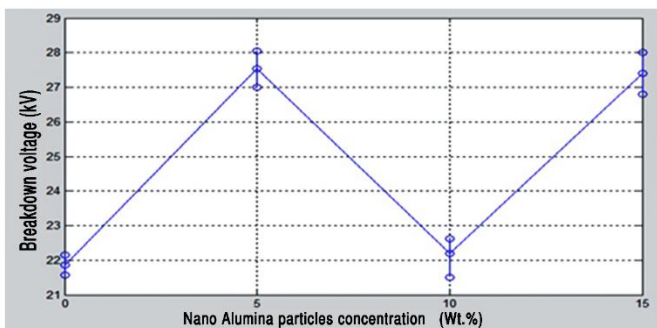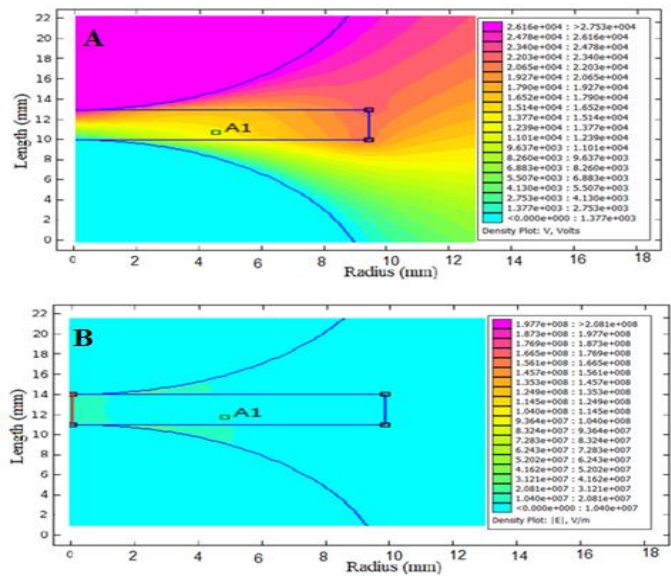

Fig.13 Voltage distribution (a) and el**e**ctric field distribution (b) in and around of porcelain sample with 5wt% nano Alumina (A1) sintered at 1200◦ c

At 1300 ℃ sintering temperature, the AC-BDV of the porcelain sample with 5wt% nano Alumina presents the highest values, which is 38.23 kV linked to the AC breakdown voltage of the blank material, which is 37.17 kV, as seen in Fig. (14). It is clear that, as the NA addition increased, the AC-BDV is decreased. The distribution of both the voltage and the electric field in and around the porcelain sample containing 5wt% NA (A1), which have the highest simulated and measured AC-BDVs, are given in Fig. (15).
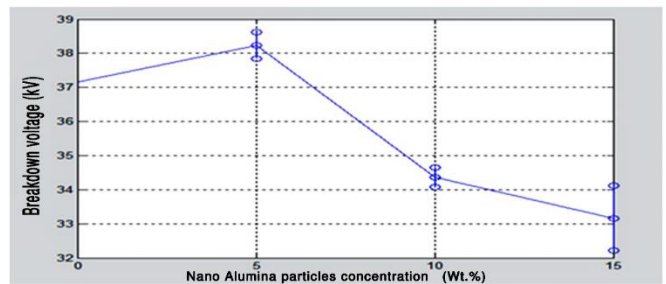

Fig.14 Average BDV of porcelain sample at different concentrations of nano Alumina sintered at 1300◦ c

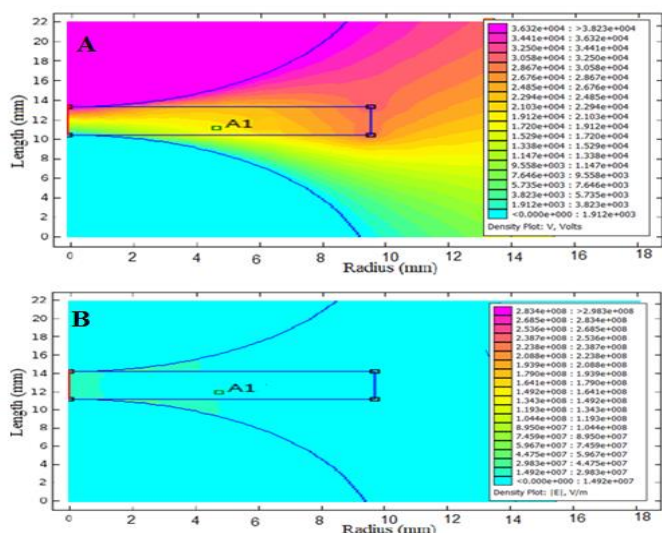Fig.12 Average BDV of porcelain sample at different concentrations of nano Alumina sintered at 1200◦ c

8

Fig.15 Voltage distribution (a) and electric field distribution (b) in and around of porcelain sample with 5wt% nano Alumina sintered at 1300 °C.

6. Conclusions

The impression of NA filler addition on the physical characteristics and electrical properties of porcelain insulator prepared from low-cost raw materials is investigated.

The findings of this investigation can be brief as follows:

1. From XED study, Addition of NA to porcelain insulator did not affect its phase composition.
2. From SEM investigation presence of NA along the porcelain matrix causes decreasing both the nano and micropores present and promote the formation of dense matrix.
3. Adding of nano-Alumina to porcelain material causes a notable rise in the bulk density, a reduction in the apparent porosity, and a loss in the water absorption at all sintering temperatures owing to its nano filling effect.
4. Porcelain specimens contain 5 wt. %NA sintered at 1300 °C present the optimum physical characteristics: greatest density (3.255 g/cm^3), lowest water absorption (0.218%), and lowest porosity (0.099 %) plus a good insulating characteristic.
5. Porcelain specimens contain 5 wt. %NA sintered at 1300 °C present the best insulating characteristics.

For porcelain samples (sintered at 1200 &1300 °C), increasing the percentage addition of NA causes notable enhancement in their insulating character.

Acknowledgments

References

 [1]   H.Kirkici, S.Mert and K.Kalyan, Nano-dielectric materials in electrical insulation application, 31st Annual Conference of IEEE Industrial Electronics Society, IECON 2005
 [2]   C. C. Okolo, O. A.Ezechukwu, C. O.Olisakwe, C. E. Ezendokwelu and Umunna, Characterization of electrical porcelain insulators from local clays. International Journal of Research–Granthaalayah , 3, 26-36 ,(2015)
 [3]   J. Liebermann, High-voltage insulators: basics and trends for producers, users and students (Fraunhofer Institute for Ceramic Technologies and Systems IKTS, Hermsdorf, 2012)
 [4]   J.E. Contreras, E.A. Rodriguez, Nanostructured insulators—a 1. Review of nanotechnology concepts for outdoor ceramic insulators. Ceram. Int. 43(12), 8545–8550 (2017)
 [5]
 [6]   C. Harper, Handbook of Ceramics, Glasses, and Diamonds. McGraw-Hill Professional ,(2001)
 [7]   E. Sánchez, and A. Moreno, Porcelain tile: Almost 30 years of steady scientific-technological evolution, Cer. Int., vol. 36, pp. 831-845,(2001)
 [8]   L.U. Anih, Indigenous manufacturer and characterization of electrical porcelain insulator. Niger. J. Technol. 24, 1 (2005)
 [9]   Zh.V.Kolpashchikova, E. V. Shcherbakova, and N. S. Kostyukov, Polarization processes in electrotechnical porcelain within a wide frequency range, Glass and Ceramics, 60.11-12, 370-373(2003)
[10]   P.Olupot Wilberforce. Assessment of ceramic raw materials in Uganda for electrical porcelain. Diss. KTH, (2006)
[11]   R.Ramesh and C. Pugazhendhi Sugumaran, Reduction of flashover in ceramic insulator with nanocomposites, 3rd International Conference on Condition Assessment Techniques in Electrical Systems (CATCON). (IEEE 2017)
[12]   J.H. Tod, A history of Electrical Porcelain Industry in the United States; Printed privately by Jack H. Todd. (1977).Available online: https://www.r-infinity.com/ebay/Electrical_Porcelain/Electrical_Porcelain_Adobe pdf (accessed on 29 January 2019).
[13]   N. Dhagat, A. Pachori, Analysis of Ceramic and Non-Ceramic Insulator under Different Levels of Salt Contamination, International Journal of Novel Research in Electrical and Mechanical Engineering , 2(2), 37-42(2015)
[14]   M. Amin, Methods for preparation of nano-composites for outdoor insulation applications. Rev. Adv. Mater. Sci 34 , 173-184 (2013)
[15]   A.Roula, K. Boudeghdegh, and N. Boufafa. Improving usual and dielectric properties of ceramic high voltage insulators. Cerâmica 55(334), 206-208 (2009)
[16]   Y. Iqbal, W. Lee, Microstructural evolution in tri-axial porcelain, J. Am. Ceram. Soc. 83, 3121–3127(2000)
[17]   Y. Iqbal, W. Lee, Fired porcelain microstructures revisited, J. Am. Ceram. Soc. 82, 3584–3590(1999)
[18]   P. Olupot, S. Jonsson, J. Byaruhanga, Study of glazes and their effects on properties of triaxial electrical porcelains from Ugandan minerals, J. Mater. Eng. Perform. 19 , 1133–1142(2010)
[19]   S.Kitouni, A. Harabi, Sintering and mechanical properties of porcelains prepared from Algerian raw materials, Cerâmica, 57(344), 453-460(2011)
[20]   V.P. Il'ina, Feldspar material from Karela for electrical engeneering, Glass and Ceram., 61(5-6), 195-197(2004)
[21]   R.A. Islam, Y.C. Chana, M. F. Islam, Structure–property relationship in high-tension ceramic insulator fired at high temperature, Mat. Sci. and Eng. , B106(2), 132-140,(2004)

9

[22] S.Kitouni, Dielectric properties of triaxial porcelain prepared using raw native materials without any additions, Balkan Journal of Electrical & Computer Engineering 2(3) (2014)

[23] D. Goeuriot, F. Belnou, P. Goeuriot and F. Valdivieso, Nanosized alumina from boehmite additions in alumina porcelain 1. Effect on reactivity and mullitisation, Ceramics Int., 30, 883-892(2004)

[24] D. Goeuriot, F. Belnou, P. Goeuriot and F. Valdivieso, Nano sized alumina from boehmite additions in alumina porcelain. Part 2: Effect on material properties, Ceramics Int., 33, 1243-1249 (2007)

[25] J. Zhuang, P. Liu, W. Dai and X. Fu, A novel application of nano anticontamination technology for outdoor high-voltage ceramic insulators, Int. J. Appl. Ceram. Technol., E46-E53 (2010)

[26] J.E. Contreras, Influencia de la inserción de nano-óxidos cerámicos sobre la microestructura y propiedades de una porcelana triaxial, PhD Thesis, FIME-UANL , Mexico (2014)

[27] V. Aigbodion, F. Achiv, O. Agunsoye and L. Isah, Evaluation of the electrical porcelain properties of alumina-silicate nano-clay, J. of the Chinese Advanced Materials Society, 4, 99-109(2015)

[28] S. L. Correia, A. P. N. Oliveira, D. Hotza and A. M. Segadaes Properties of Tri-axial Porcelain Bodies: Interpretation of Statistical Modeling, J. Am. Ceram. Soc. 89 (11), 3356–3365(2006)

[29] K.Belhouchet, A.Bayadi, H.Belhouchet, and M.Romero, Improvement of mechanical and dielectric properties of porcelain insulators using economic raw materials., Boletín de la Sociedad Española de Cerámica y Vidrio , 58(1)28-37(2019)

[30] B. Kumar Paul, K. Haldar, D. Roy, B. Bagchi, A. Bhattacharya, S. Das, Abrupt change of dielectric properties in mullite due to titanium and strontium incorporation by sol–gel method, J. Adv. Ceram. 3 (4) ,278–286(2014)

[31] C.R. Gautam, A. Madheshiya, R. Mazumder, Preparation, Crystallization, microstructure and dielectric properties of lead bismuth titanate borosilicate glass ceramics, J. Adv. Ceram, 3 ,194–206(2014)

[32] A.Krell, S.Schadlich, Nano indentation hardness of submicrometer alumina ceramics. Mater. Sci. Eng A 307 , 172–181(2001)

[33] H.Einaga, S. Futamura, Comparative study on the catalytic activities of alumina- supported metal oxides for oxidation of benzene and cyclohexane with ozone. React. Kinet. Catal. Lett. 81 (1), 121–128(2004)

[34] P.L Sun, S.P. Wu, T.S Chin, Melting point depression of tin nanoparticles embedded in a stable alpha-alumina matrix fabricated by ball milling. Mater. Lett.144, 142–145(2015)

[35] P. S.Behera, R. Sarkar, and S. Bhattacharyya, Nano alumina: a review of the powder synthesis method, Interceram-International Ceramic Review 65(1-2) , 10-1(2016)

[36] ASTM C20, Standard Test Methods for Apparent Porosity, Water Absorption, Apparent Specific Gravity and Bulk Modulus of Burned Refractory Brick and Shapes (ASTM International, West Conshohocken, 2010)

[37] ASTM C356-10, Standard Test Method for Linear Shrinkage of Preformed High-Temperature Thermal Insulation Subjected to Soaking Heat (ASTM International, West Conshohocken, 2010)

[38] G. Dutta, K. P. Hembram, G. M. Rao, and U. V. Waghmare ,Effects of O vacancies and C doping on dielectric properties of ZrO2Zr O2: a first-principles study, Applied Physics Letters, 89(20), Article ID202904(2006)

[39] M.M.Selima, S.A. Hassanb, M.R.A. Rezkc and N. M Deraza, Characterization of Cordierite Synthesized from Egyptian Kaolin and Talc., Egyptian Journal of Chemistry 53(4), 553-563(2010)

[40] L.Fernandes, and R. Salomão, Preparation and characterization of mullite-alumina structures formed" in situ" from calcined alumina and different grades of synthetic amorphous silica. Materials Research 21(3),(2018)

[41] A.Aras, and F.Kristaly ,α-Cristobalite formation in ceramic tile and sewage pipe bodies derived from Westerwald ball clay and its effect on elastic-properties, Applied Clay Science, 178, 105126(2019)

[42] M.S. Conconi, M.R.Gauna, M.F.Serra, G.Suarez, E.F.Aglietti, and N.M. Rendtorff, Quantitative firing transformations of a triaxial ceramic by X-ray diffraction methods. Cerâmica, 60(356), 524-531(2014)

[43] S.Q. Yang, P. Yuan, H.P. He, Z.H. Qin, Q. Zhou, J.X. Zhu, D. Liu, Effect of Reaction Temperature on Grafting of aminopropyltriethoxysilane (APTES) onto kaolinite, J. Appl. Clay Sci. 62 ,8–14(2012)

[44] Z.L.Ntah, R.Sobott, B.Fabbri, and K.Bente, Characterization of some archaeological ceramics and clay samples from Zamala-Far-northern part of Cameroon (West Central Africa). Cerâmica, 63(367), 413-422(2017)

[45] S. A. Kayani, Mineralogical and Thermal Analyses of a Bangle Shard from Harrappa, an Indus Valley Settlement in Pakistan, Analele Stiintifice ale Universitatii "Al. I. Cuza" din Iasi, Seria Geologie, 2011

[46] N. El-Mehalawy, M. Awaad, T. Eliyan, M. A. Abd-Allah and S. M. Naga, , Electrical Properties of ZnO/alumina Nano-composites for high voltage transmission line insulator, Journal of Materials Science: Materials in Electronics, 29 ,13526-13533(2018)

[47] N.S.Mehta, P.K. Sahu, P. Tripathi, R. Pyare, and M.R.Majhi, Influence of alumina and silica addition on the physico-mechanical and dielectric behavior of ceramic porcelain insulator at high sintering temperature, boletín de la sociedad española de cerámica y vidrio 57(4), 151-159(2018)

[48] A.O.Oladiji, J.O.Borode, B.O. Adewuyi, and I.O.Ohijeagbon, Development of porcelain insulators from locally sourced materials. USEP: Journal of Research Information in Civil Engineering 7(1) , 47-58 (2010)

[49] J.E. Contreras, M. Gallaga, and E. A. Rodriguez, Effect of nanoparticles on mechanical and electrical performance of porcelain insulator, IEEE Conference on Electrical Insulation and Dielectric Phenomena (CEIDP). (IEEE 2016)

[50] V. Rajendran, P. Manivasakan, P. Rauta, B. Sahu, P. Sahu, and B. Panda, Effect of TiO2 nanoparticles on properties of silica refractory, J. of the American Ceramic Society, 93, 2236-2243 (2010)

[51] N. M.Mohammed, and L. J. Ibraheim,Manufacture of porcelain insulator from Iraqi raw material and studying the effect of nano alumina additives on the dielectric properties, AIP Conference Proceedings, 2213(1). AIP Publishing LLC(2020)